JOURNAL OF AGRICULTURAL AND FOOD CHEMISTRY

J. Agric. Food Chem. **2005,** *53,* 6027−6034 **6027**

Biochemical and Biophysical Changes Induced by Fungicide Sodium Diethyl Dithiocarbamate (SDD), in Phytocystatin Purified from *Phaseolus mungo* (Urd): A Commonly Used Indian Legume

SANDEEP SHARMA, FOUZIA RASHID, AND BILQEES BANO*

Department of Biochemistry, Faculty of Life Sciences, Aligarh Muslim University, Aligarh-202002 (U. P.), India

Phytocystatins are the plant thiol protease inhibitors involved in several reaction mechanisms of the plant system like regulation of proteolytic activity and storage of proteins. Biochemical and biophysical changes induced by fungicide SDD in phytocystatin purified from *Phaseolus mungo* have been investigated in terms of mass spectroscopy, Fourier transform infrared spectroscopy, and fluorescence spectroscopy, at pH 7.0, with varying fungicide concentrations (1−9 mM) and a time of incubation ranging from 2 to 8 h at 37 °C, with a fixed cystatin concentration (1.5 mM). Reactive oxygen species responsible for inhibitor damage were also investigated, and thiourea was found to scavenge the free radicals generated by SDD. FTIR analysis indicates a significant conformational transition from α-helix to β-sheet structure; quenching of fluorescence is evident by fluorescence spectroscopy. The activity assay showed a decrease in inhibitory activity, as well as a fragmentation of the inhibitor was observed in electrophoresis. Results obtained implicate that exposure of phytocystatins to SDD involves physicochemical changes in cystatins leading to damage and a decrease in the activity of the inhibitor.

KEYWORDS: SDD; Fourier transform infrared spectroscopy; fluorescence spectroscopy; protease inhibitor; proteins

INTRODUCTION

Pesticide is any substance intended for preventing, repelling, or destroying any pests. This definition includes herbicides, which are used to kill unwanted plants, insecticides, and fungicides, which are specifically used to kill molds, insect pests, and fungi. SDD is a fungicide used widely to protect fruits, grains, crops, and vegetables; as a consequence of low price and easy availability, the use of compounds such as SDD (sodium diethyl dithiocarbamate) has been widely expanded, and without its use, the agricultural yield of field crops would drop by 30−50% (*1*). The extensive use of fungicides in agricultural practice is one of the most important ecotoxicological problems in developing as well as in the developed countries. SDD is absorbed in plant products. When such compounds are consumed by animal systems, they reach through the bloodstream to various parts of the body and affect some proteins (*2*). Mammalian exposure to dithiocarbamates such as SDD leads to gonadal toxicity, a decrease in the level of different proteins, and an increase in the thyroid concentration (*3*). Furthermore, long-term exposure to dithiocarbamates has been associated with Parkinsonism and an increased risk of neurocognitive impairment (*4*).

The study of the interaction of SDD with proteins is very important because this interaction has been reported to induce morphological changes in plants such as root-growth retardation (*5*), defects in the storage of proteins, regulation of proteolytic activity, and apoptosis (*6*, *7*, *8*). Apoptosis or plant programmed cell death has been implicated in several processes such as xylogenesis (*9*), some forms of senescence, and in the attack response of pathogens (*10*, *11*).

Thiol proteinase inhibitors are found ubiquitously in animal and plant systems. The known proteins of the cystatin superfamily have been divided into three families, namely, stefins (type-I cystatins), cystatins (type-II cystatins), and kininogens, found only in mammalian plasma (*12*, *13*). During the past decade, a fourth group belonging to the cystatin superfamily has emerged, that is, the plant cystatins. Homology searches show that some plant cystatins resemble family I cystatin and some resemble family II cystatins of animal origin (*14*), and both plant and animal cystatins are shown to be evolved from a cognate ancestrol gene (*15*, *16*).

Phytocystatins such as oryzacystatin I and II have been reported to show antiviral effect against polio and herpes simplex virus (HSV-I) (*17*, *18*), which is a potential biotechnological

* To whom correspondence should be addressed: Department of Biochemistry, Faculty of Life Sciences, AMU, Aligarh. E-mail: sharma_mos@yahoo.co.in. Telephone: +91-571-2700857. Fax: +91-571-2702758.

10.1021/jf050580p CCC: $30.25
Published on Web 07/02/2005

application of phytocystatins. Furthermore, purified sugarcane cystatin is found to inhibit the growth of filamentous fungus *Trichoderma reesi* (*19*).

In the present study, phytocystatin has been purified from a natural, easily available, and a cheap source, *Phaseolus mungo* (Urd). It resembles the properties of both the type-I and type-II cystatins of the mammalian system (*14*). This is the first report that indicates the biochemical and biophysical changes in phytocystatins because of the interaction with SDD.

Although the effect of SDD on phytocystatin might not be specific but because the investigations have been done on cystatin purified to the extent of homogeneity, studies on the interaction of phytocystatins with SDD are relevant and are of great biochemical importance.

2. MATERIALS AND METHODS

Materials. SDD was purchased from Sigma. Other chemicals including free-radical scavengers were of analytical grade.

Methods. *2.1. Purification of Inhibitor.* Cystatin I and II were purified by the modification of the method of Juwen and Haard (*20*). A total of 100 g of Urd seeds were soaked in 25 mM sodium phosphate buffer (pH 7.0) and 0.15 M sodium chloride. This preparation was kept overnight at 4 °C. Seeds were then homogenized and subjected to centrifugation in a Sigma cooling centrifuge (Japan) at 4000 rpm for 20 min at 4 °C. The supernatant thus collected was saturated with 40% ammonium sulfate and then centrifuged at 8000 rpm for 20 min, and the supernatant thus collected was made 70% saturated with ammonium sulfate. After 4 h, the pellet was recovered by centrifugation and dissolved in 10 mL of 25 mM sodium phosphate buffer (pH 7.0). The pellet thus obtained was extensively dialyzed against several changes of the same buffer at 4 °C to remove ammonium sulfate. The dialyzed sample was then loaded on a sephacryl S-100 gel-filtration column. Fractions (5 mL) were collected and assayed for cystatin inhibitory activity and protein concentration.

2.2. Mass Spectrometry: Matrix-Assisted Laser Desorption−Time-of-Flight (MALDI−TOF) Analysis of Cystatin 1 and 2. To further check the purity, cystatin 1 and 2 were again loaded on sephacryl S-100 gel-filtration column, and it was eluted with sodium phosphate buffer (25 mM, pH 7.0). Samples were then freeze-dried, desalted, and prepared for analysis on a Voyager Bioworkstation (Perspective Biosystems). The samples were dissolved in 1.0% trifluoroacetic acid, and the matrix sinapinic acid (a saturated solution dissolved in acetonitrile/0.1% TFA, 1:1, v/v, Sigma chemicals) was added. This preparation was then vortexed, and 1.2 mL (1 mg/mL) of each cystatin 1 and 2 was applied on the sample plate. The spectrophotometer equipped with delayed extraction system accessory was operated in a linear mode. Sample ions were evaporated using a N_2 laser at 330 nm wavelength and accelerated at a potential of 20 kV with a delay of 134 ns. Around 150 shots of 3 ns pulse width laser light were required to ionize the sample. Finally, the signal was digitized at a rate of 480 MHz.

2.3. Electrophoresis. Polyacrylamide gel electrophoresis and SDS−PAGE were performed at room temperature in the buffer system by the method of Laemmli (*21*). In SDS−PAGE, samples were reduced with 0.1 M β-mercaptoethanol. The gels were silver-stained, and the percentage of the gel was 7.5% for PAGE and 12.5% for SDS−PAGE.

2.4. Investigation of the Cystatin Autolysis. The autolysis of cystatin 1 and 2 was checked at different incubation times. For this investigation, both the cystatins were incubated for 0, 2, 4, 6, 8, 12, and 24 h at 37 °C in sodium phosphate buffer (pH 7.0, 25 mM). After each incubation period, samples were analyzed by 7.5% PAGE, the gels were silver-stained, and cystatin inhibitory activity was monitored by the modification of the method of Kunitz.

2.5. Effect of SDD on Cystatins (Thiol Protease Inhibitory Activity). The direct effect of SDD on the thiol proteinase inhibitory activity of purified cystatin 1 and 2 was investigated by a modification of the method of Kunitz. For this assay, cystatin 1 and 2 (1.5 mM) were incubated with SDD in different concentrations (0.5, 1, 1.5, 3, 6, and 9 mM) prior to incubation with papain, for 2, 4, 6, and 8 h at 37 °C in 25 mM sodium phosphate buffer (pH 7.0). Then, papain (4 mM) was activated for 10 min (using 0.2 M EDTA and 0.5 M cysteine). It was then incubated with cystatin SDD complex for an additional 10 min. This complex was then incubated with casein for 30 min at 37 °C, and the reaction was stopped by the addition of 10% trichloroacetic acid. Acid-insoluble material was removed by centrifugation at 3000 rpm for 15 min. The supernatant was analyzed for acid-soluble peptides with Folin's phenol reagent by the method of Lowry (*22*). Papain inhibitory activity was also investigated by the same method except that inhibitor was absent. The experiment was repeated 3 times, and statistical significance was conducted employing one-way ANOVA. A probability level of $p < 0.05$ was selected for indicating statistical significance. The control had a buffer in equal volume in place of SDD.

2.6. Fluorescence Spectroscopy. For fluorescence measurements, cystatin 1 and 2 (1.5 mM) were incubated for 2, 4, 6, and 8 h at 37 °C with SDD (1−9 mM). Fluorescence emission spectra were taken after each incubation in the wavelength range of 300−400 nm. The equipment used for this investigation was Shimadzu RF-1501 spectrofluorophotometer (Japan), and spectra were recorded using a xenon arc lamp as the light source. For the sake of accuracy, the average of three scans was taken.

2.7. Fourier Transform Infrared Spectroscopy. Infrared spectroscopy was done to see the conformational changes observed during cystatin and SDD interaction. The spectra was truncated between 1740 and 1520 cm^{-1} and baseline corrected. The equipment used was NICOLET (ESP) 560 spectrophotometer equipped with a transmission OMNIC ESP 5.1 software and a DTGS detector; data was analyzed and quantitated using Grams 32 software. Original spectra of native cystatins (cystatin 1 and 2) along with cystatin co-incubated with SDD at 37 °C were taken with a fixed concentration of cystatin (1.5 mM) and an increasing concentration of SDD (1−9 mM) with a resolution of 4 cm^{-1} and 128 scans. The changes in peak frequency and intensity were then assigned to conformational changes within the protein (*23*).

2.8. Free-Radical Study. Interaction of SDD with cystatin was also analyzed for any possible involvement of free radicals after co-incubating SDD with cystatin and then by adding different free-radical scavengers (thiourea, sodium azide, ascorbic acid, and potassium iodide). For this investigation, free-radical scavengers (100 mM) were incubated with fungicide SDD (3 mM) at 37 °C, while the concentration of cystatin 1 and 2 was kept at 1.5 mM.

3. RESULTS AND DISCUSSION

All of the investigations done in this study were also carried out at zero time controls, which showed no loss in inhibitory activity, as well as no fragmentation or conformational change in the cystatins was observed after it was incubated with SDD.

3.1. Purification of the Inhibitor. The purified inhibitors were obtained as peak 1 (cystatin 1) and peak 2 (cystatin 2) respectively from S-100 gel-filtration analysis (results not shown); the inhibitor migrated as a single band on native PAGE indicating charge homogeneity. The SDS−PAGE analysis in reducing conditions (that is the sample containing β-mercaptoethanol) gave the molecular mass of 19 and 17 kDa, respectively. SDS−PAGE in reducing as well as nonreducing conditions (in the absence of β-mercaptoethanol) demonstrated the lack of subunit structure, which shows that cystatins are homogeneous in SDS−PAGE and that both the cystatins are constituted by a single polypetide chain.

3.2. Mass Spectrometry (MALDI−TOF Analysis). MALDI−TOF analysis is one of the most recent and sophisticated techniques through which accurate molecular weights can be obtained easily in a short time period. The molecular mass of cystatin as analyzed by mass spectrometry is found to be 19 124.36 and 17 510.22 Da for cystatin 1 and 2, respectively, which is very similar to that determined by SDS−PAGE (under reducing condition). Parts **A** and **B** of **Figure 1** demonstrates the molecular weight determination by mass spectrometry.

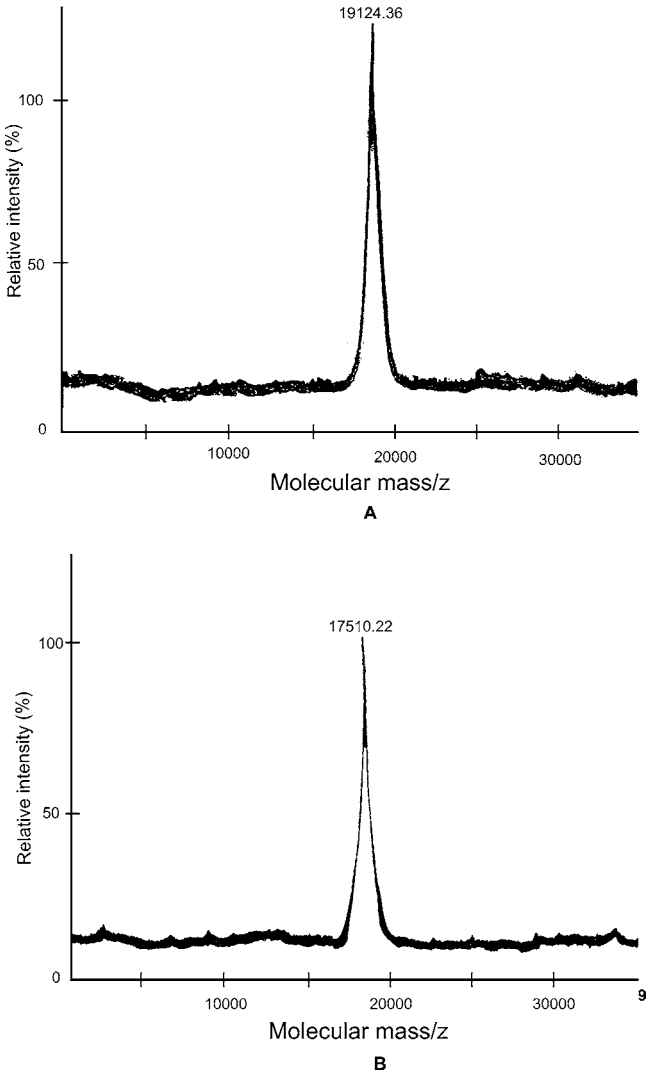

Figure 1. A and B show the molecular weights determined by mass spectrometry (MALDI–TOF). A represents cystatin 1, while B represents cystatin 2.

3.3. Gel Electrophoresis. The effects of incubation of SDD with cystatin are presented in parts **A**−**D** of **Figure 2**. Parts **A**−**D** of **Figure 2** illustrate the effect of SDD toxicity on purified cystatin 1 and 2. Native PAGE was done to see if there was any change in the electrophoretic behavior of the inhibitor after its interaction with SDD. Parts **A** and **B** of **Figure 2** show the electrophoretic profile of cystatin 1 and 2 incubated with SDD (1, 1.5, and 3 mM) for 2 and 4 h, respectively. It is observed that at low concentration (1 mM) of SDD the bands are more intense for cystatin 1 (lane b in **Figure 2A**) for 2 h of incubation, as compared to cystatin 2 (lane b in **Figure 2B**). This shows that the interaction has caused less fragmentation in cystatin 1 as compared to cystatin 2. As the concentration of the SDD is increased (1.5 and 3 mM) with the time of incubation (2−4 h), the fragmentation of cystatins increases successively (lanes c−g in parts **A** and **B** of **Figure 2**). The results of cystatin 1 and 2 incubated for 6−8 h are shown in parts **C** and **D** of **Figure 2**. As compared to parts **A** and **B** of **Figure 2**, the electrophoretic mobility in parts **C** and **D** of **Figure 2** clearly demonstrates that the inhibitor is fragmented to a higher extent at 6 and 8 h of incubation. At 3 mM concentration of SDD and at an incubation time of 8 h, the extent of damage to cystatin is such that bands are poorly visible and even migrate to a different position as compared to that of native cystatin in lane a in parts

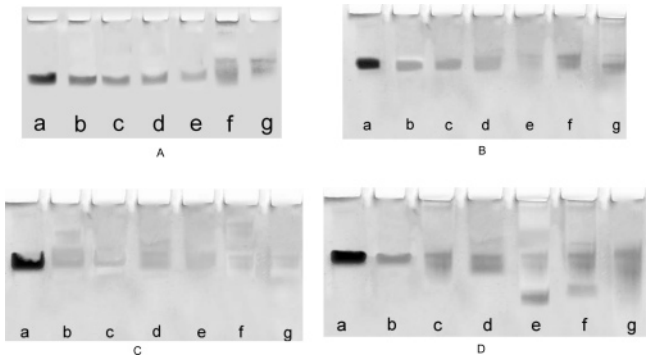

Figure 2. (A and B) Polyacrylamide gel electrophoresis of cystatin after co-incubating SDD with a fixed concentration of cystatin (1.5 mM) for 2 and 4 h at 37 °C. A represents cystatin 1, and B represents cystatin 2. Lane a, untreated cystatin (1.5 mM). Lane b, cystatin and SDD (1 mM) co-incubated for 2 h. Lane c, cystatin and SDD (1 mM) co-incubated for 4 h. Lane d, cystatin and SDD (1.5 mM) co-incubated for 2 h. Lane e, cystatin and SDD (1.5 mM) co-incubated for 4 h. Lane f, cystatin and SDD (3 mM) co-incubated for 2 h. Lane g, cystatin and SDD (3 mM) co-incubated for 4 h. (C and D) Polyacrylamide gel electrophoresis of cystatin after co-incubating SDD with a fixed concentration of cystatin (1.5 mM) for 6 and 8 h at 37 °C. C represents cystatin 1, and D represents cystatin 2. Lane a, untreated cystatin (1.5 mM). Lane b, cystatin and SDD (1 mM) co-incubated for 6 h. Lane c, cystatin and SDD (1 mM) co-incubated for 8 h. Lane d, cystatin and SDD (1.5 mM) co-incubated for 6 h. Lane e, cystatin and SDD (1.5 mM) co-incubated for 8 h. Lane f, cystatin and SDD (3 mM) co-incubated for 6 h. Lane g, cystatin and SDD (3 mM) co-incubated for 8 h.

A−**D** of **Figure 2**. **Figure 2** shows that fragmentation of cystatin 1 and 2 increases gradually with an increase in the SDD concentration, and it can be said that at a lower SDD concentration the effect is insignificant. At 6 and 9 mM concentrations of SDD, the bands vanished completely (results not shown). Thus, intensity of the cystatin band at different incubation times as compared to native cystatin (lane a) gives a clear picture showing the fragmentation of purified cystatin in the presence of SDD. Furthermore, the progressive change in the electrophoretic pattern of cystatins could also be due to a conformational change or cystatin denaturation because of incubation of cystatin at 37 °C for 6−8 h.

3.4. Investigation of the Cystatin Autolysis at Different Incubation Times. This investigation was done to see if fragmentation of cystatin is due to its autolysis. Cystatin 1 and 2 (1.5 mM) were incubated for 0, 2, 4, 6, 8, 12, and 24 h at 37 °C. The results analyzed by PAGE indicate that there was no change in cystatin migration even at 24 h of incubation, which confirms that both the cystatins are stable after 24 h of incubation. The cystatin inhibitory activity was also monitored in the samples after each incubation to see if there is any decrease in cystatin inhibitory activity after 24 h of incubation, and it was found that there was no change in the inhibitory activity of cystatins.

3.5. Effect of SDD on Cystatin Inhibitory Activity. To establish whether SDD had a direct effect on cystatin, the inhibitory activity of papain was determined after prior incubation of cystatin with SDD. Results are shown in **Table 1**. Statistical analysis (one-way ANOVA) indicates a significant loss in thiol protease inhibitory activity after the interaction of the inhibitor with SDD, and this decrease in activity was more pronounced with an increase in the concentration as well as incubation time with SDD. This tremendous loss in inhibitory activity is in accordance with the electrophoretic pattern (**Figure**

Table 1. Percent Loss in the Thiol Protease Inhibitory Activity after Co-incubating Cystatin (1.5 mM) with Varying Concentrations of SDD (0.5, 1.0, 1.5, 3.0, 6.0, and 9 mM) and Varying Incubation Times at 2, 4, 6, and 8 h and 37 °C[a]

concentration of SDD (mM)	2 h incubation		4 h incubation		6 h incubation		8 h incubation	
	cystatin 1	cystatin 2	cystatin 1	cystatin 2	cystatin 1	cystatin 2	cystatin 1	cystatin 2
0.5	76.1 ± 153	73.19 ± 0.098	72.06 ± 0.032	71.95 ± 0.032	71.29 ± 0.023	70.26 ± 0.133	43.07 ± 0.067	44.57 ± 0.035
1.0	72.87 ± 0.146	71.02 ± 0.016	70.09 ± 0.050	69.26 ± 0.136	70.09 ± 0.044	69.78 ± 0.021	31.71 ± 0.147	29.95 ± 0.036
1.5	71.90 ± 0.052	69.60 ± 0.300	67.07 ± 0.68	64.19 ± 0.099	60.05 ± 0.036	61.32 ± 0.003	26.36 ± 0.136	22.97 ± 0.18
3.0	63.07 ± 0.035	62.01 ± 0.007	49.08 ± 0.042	43.52 ± 0.294	41.09 ± 0.107	37.89 ± 0.007	12.95 ± 0.023	12.44 ± 0.026
6.0	50.93 ± 0.231	49.55 ± 0.309	41.15 ± 0.078	41.97 ± 0.030	28.00 ± 0.00	27.47 ± 0.260	8.72 ± 0.015	10.22 ± 0.008
9.0	47.23 ± 0.125	45.07 ± 0.046	33.64 ± 0.046	32.94 ± 0.032	11.11 ± 0.006	13.10 ± 0.052	3.61 ± 0.012	4.20 ± 0.008

[a] Inhibitory activity is calculated with the control taken as 100. All data are expressed as mean ± SE for three different sets. Statistical significance was conducted employing one-way ANOVA. A probability level of $p < 0.05$ was selected as indicating statistical significance.

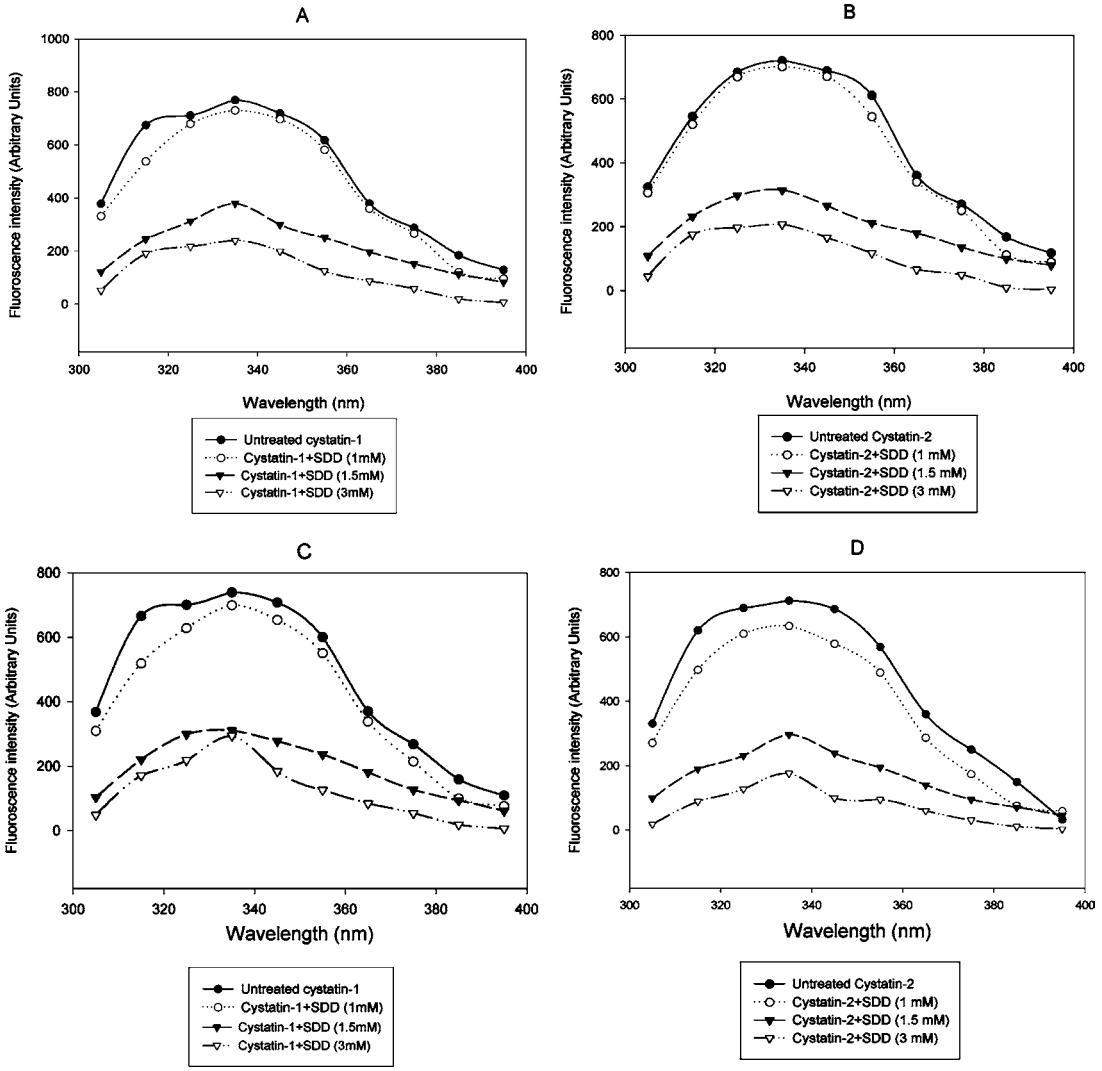

Figure 3. (A and B) Fluorescence emission spectra of cystatin (1.5 mM) in the absence of SDD (uppermost curve) and in the presence of increasing SDD concentration (1, 1.5, and 3 mM) obtained in 25 mM sodium phosphate buffer (pH 7.0) after co-incubating SDD with cystatin for 2 h at 37 °C. A represents emission spectra of cystatin 1, and B represents emission spectra of cystatin 2. (C and D) Fluorescence emission spectra of cystatin (1.5 mM) in the absence of SDD (uppermost curve) and in the presence of increasing SDD concentration (1, 1.5, and 3 mM) obtained in 25 mM sodium phosphate buffer (pH 7.0) after co-incubating SDD with cystatin for 4 h at 37 °C. C represents emission spectra of cystatin 1, and D represents emission spectra of cystatin 2.

2), which demonstrates a fragmentation/conformational change of the inhibitor, thus providing strong evidence of the deletorious impact of fungicide on cystatin. A similar assay was done to see the direct effect of SDD on the activity of papain. The decrease in the enzyme activity for 8 h of incubation with 9 mM concentration of SDD was only 2%, which is insignificant. This implicates that SDD was not able to produce any change in papain, and whatever fragmentation of cystatin is observed is due to the impact of SDD on cystatin.

3.6. Fluorescence Spectroscopy. Fluorescence spectroscopy was performed to investigate the spectral changes after the interaction of cystatin with SDD. The cystatin and SDD solutions were incubated for 2 and 4 h, and after each incubation, fluorescence spectra were taken. The excitation wavelength was

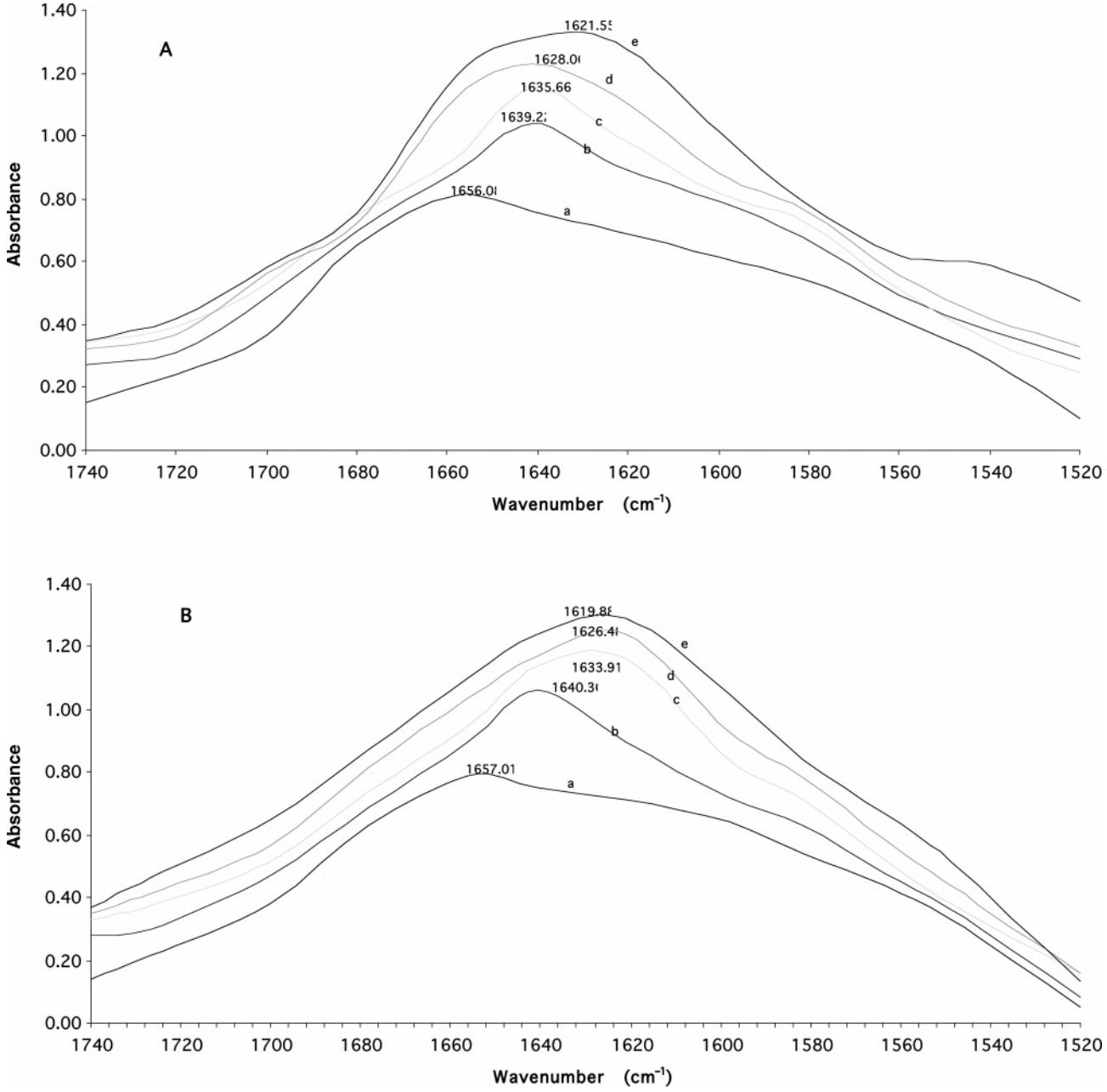

Figure 4. (A and B) FTIR spectra of cystatin 1 and 2 co-incubated with SDD at 37 °C. The concentration of cystatin 1 and 2 was kept fixed (1.5 mM). A represents cystatin 1, while B represents cystatin 2. In both A and B, (a) native cystatin (1.5 mM), (b) cystatin co-incubated for 2 h with SDD (1.5 mM), (c) cystatin co-incubated for 4 h with SDD (1.5 mM), (d) cystatin co-incubated for 2 h with SDD (3 mM), and (e) cystatin co-incubated for 4 h with SDD (3 mM).

284 nm, and emission spectra were taken in the wavelength range of 300−400 nm with a slit width of 10 nM. **Figure 3** illustrates the results of fluorescence emission spectra. The concentration of cystatin 1 and 2 was fixed (1.5 mM), while the SDD concentration was varied as 1, 1.5, and 3 mM. **Figure 3** shows the quenching of fluorescence intensity with an increasing concentration of SDD. At a low SDD concentration (1.5 mM), minimal quenching occurs, but as the concentration of SDD is increased, quenching increases successively. Quenching of fluorescence is almost the same in cystatin l and 2. The fluorescence emission spectra of both the cystatins is summarized in parts **A**−**D** of **Figure 3**. At a concentration of 6 and 9 mM of SDD, cystatin fluorescence was fully quenched (results not shown).

3.7. Fourier Transform Infrared Spectroscopy (FTIR). FTIR spectroscopy was done to analyze the conformational changes during cystatin−SDD interaction. The results further confirm the damage caused to cystatin as shown in previous investigations. In the IR spectra of proteins, the secondary structure is most clearly reflected by the amide I and II bands, particularly the former (*24*−*26*); the amide I band absorbs at 1657 cm^{-1} (mainly a C═O stretch), and the amide II band absorbs at 1542 cm^{-1} (C−N stretching coupled with N−H bending modes) (*27*, *28*). It has also been reported that, for a native protein, the amide I component for the α-helical structure locates at 1656 ± 2 cm^{-1} and the band components for the β-sheet structure should locate between 1622 and 1642 cm^{-1} (lower wavenumber β-sheet bands) and between 1690 and 1698 cm^{-1} (higher wavenumber β-sheet bands) (*24*−*26*, *29*). **Figure 4** shows the original spectra of native (untreated cystatin) along with cystatin co-incubated for 2 and 4 h consecutively with SDD (1.5 and 3 mM). Quantitative analysis of the protein secondary

Table 2. Secondary Structure Determination of Native Cystatin and Its SDD Complexes in Sodium Phosphate Buffer at pH 7.0, 25 mM), with Varying Concentrations of Fungicide at Different Incubation Periods[a]

amide I components (cm^{-1})	native cystatin values in %		1.5 mM cystatin–SDD (2 h incubation) values in %		1.5 mM cystatin–SDD (4 h incubation) values in %		3 mM cystatin–SDD (2 h incubation) values in %		3 mM cystatin–SDD (4 h incubation) values in %	
	C-1[b]	C-2[c]	C-1	C-2	C-1	C-2	C-1	C-2	C-1	C-2
1692–1680, β anti	7 ± 1	7.8 ± 1	13.2	12.5	14.8	11.7	15.4	11.3	18.8	15.5
1673–1666, β turn	8 ± 1	6.7 ± 1	14.7	12.9	14.1	12.8	13.0	11.7	13.1	12.8
1658–1650, α helix	58.0 ± 2	56.5 ± 3	46.5	45.0	44.1	44.0	38.2	37.5	37.0	37.2
1640–1615, β sheet	27 ± 1	29 ± 2	27.2	29.5	27.7	29.4	28.6	31.2	29.0	31.6

[a] The mean deviation was from ±1 to ±2 for the free cystatin and fungicide complexes. [b] C-1 = cystatin 1. [c] C-2 = cystatin 2.

structure for native cystatin (1 and 2) and SDD-treated cystatin is given in **Table 2**. Cystatin 1 contained the major α helix at 58%, β sheet at 27%, turn structure at 8%, and β antiparallel at 7%. Cystatin 2 contained α helix at 56.5%, β sheet at 29%, turn structure at 6.7%, and β antiparallel at 7.8%. Upon fungicide interaction, the α-helix structure was reduced from 58 to 46.5−37% in cystatin 1 and from 56.5 to 45−37.2% in cystatin 2. The reduction of the α-helix in favor of the β-sheet structure is indicative of the partial unfolding of the inhibitor in the presence of SDD. A similar conformational transition from α-helix to β-sheet structure was observed for the myelin protein upon heating the protein at 35 °C (*30*). Furthermore, from the data obtained in **Table 2**, it was found that, at a concentration of 1.5 mM SDD and at 2 h of incubation, the percent increase in β antiparallel is 88.57 and 60.25%, and the increase in β-turn is 83.75 and 92.53%, while the α-helical structure shows a reduction of 19.82 and 20.35% with a 0.74 and 1.72% increase in the β-sheet structure, for cystatin 1 and 2, respectively. At a 3 mM SDD concentration and at an incubation time of 4 h, an increase in β antiparallel is 168.57 and 98.71%, an increase in β turn is 63.75 and 91.04%, and a decrease in α-helical structure is found to be 36.2 and 34.15%, while an increase in the β-sheet structure is 7.4 and 8.96% respectively for cystatin 1 and 2. The percent increase/decrease is calculated in comparison to the values obtained for native cystatins.

Thus, the results summarized in parts **A** and **B** of **Figure 4** and **Table 2** further confirm the damage caused to cystatin as evidenced by a significant shift in the peak intensity, i.e., from 1656.08 to 1621.55 (cystatin 1) and 1657.01 to 1619.88 (cystatin 2) and significant changes in the structure of cystatin from that of α helix to β structure (lower wavenumber β-sheet bands), after co-incubating cystatin (1 and 2) for 4 h with SDD (3 mM).

3.8. Effect of Free-Radical Scavengers on the Interaction of SDD with Cystatin. It is well-known that the fungicide toxicity of proteins is due to free-radical generation (*31*). Exposure of plants to a variety of adverse conditions such as pesticide treatment leads to free-radical production mediated by catalytic Fe. It has also been reported that catalytic Fe increases free-radical generation steadily in plants exposed to pesticides (*32*). Iron has a pivotal role in free-radical chemistry in all organisms. It is present in plant extracts and legumes (*33*). Plants are reported to contain all of the basic components required for the *in vitro* production of hydroxyl radicals, which are formed through a Fenton reaction catalyzed by iron present in plants (*32*). Thus, it was thought worthwhile to check the possible involvement of reactive oxygen species generated by SDD in the conformational change and inactivation or fragmentation of cystatins; with this aim, the effect of free radical scavengers was investigated.

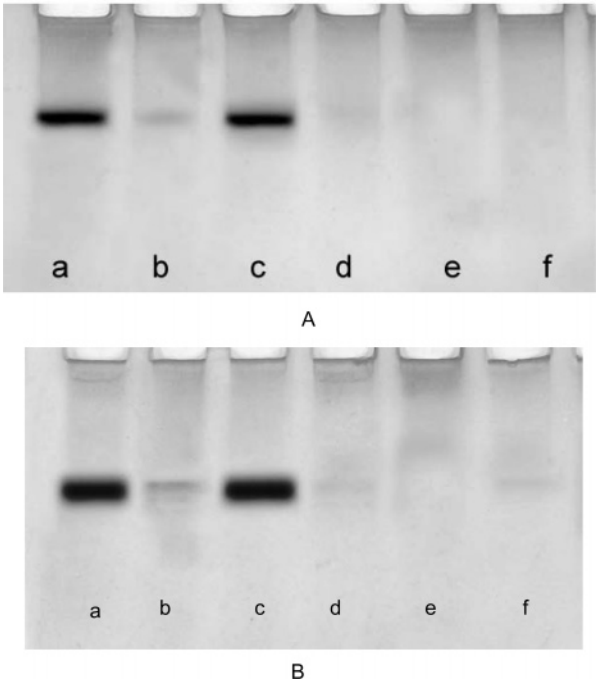

Figure 5. (A and B) Effect of different free-radical scavengers on cystatin (1.5 mM) co-incubated with SDD for 4 h at 37 °C. A represents cystatin 1, while B represents cystatin 2. Lane a, native cystatin (1.5 mM). Lane b, cystatin co-incubated with SDD (3 mM). Lane c, cystatin co-incubated with SDD (3 mM) and thiourea (100 mM). Lane d, cystatin co-incubated with SDD (3 mM) and sodium azide (100 mM). Lane e, cystatin co-incubated with SDD (3 mM) and potassium iodide (100 mM). Lane f, cystatin co-incubated with SDD (3 mM) and ascorbic acid (100 mM).

For this investigation, cystatin 1 and 2 (1.5 mM) were co-incubated for 2 h with SDD (3 mM) alone as well as with different free-radical scavengers such as ascorbic acid, thiourea, potassium iodide, and sodium azide (each with a concentration of 100 mM). This investigation was done to analyze the kind of free radical involved in fragmentation of cystatin. Parts **A** and **B** of **Figure 5** show the scavenging effect of the free radical by various scavengers for cystatin 1 and 2, respectively. In lane a of parts **A** and **B** of **Figure 5** is the native protein (cystatin 1 and 2), while in lane b of parts **A** and **B** of **Figure 5**, native protein is co-incubated with SDD. The results indicate that cystatin 1 and 2 attain the position of the native band when incubated for 4 h with 3 mM of SDD in the presence of thiourea (100 mM). Because thiourea is a scavenger of hydroxyl radicals, generation of hydroxyl radicals is established. In lane c in parts **A** and **B** of **Figure 5**, cystatins are degraded in all other lanes except lane c. This is because of the fact that scavengers present in other lanes (lanes d−f), i.e., sodium azide, potassium iodide, and ascorbic acid, are scavengers of superoxide anion and singlet

oxygen, which were unable to produce any scavenging effect. Thus, it shows that thiourea is involved in scavenging hydroxyl radicals generated by SDD. Production of hydroxyl radicals has also been reported in radish seeds because of the Fenton-type reaction (*34*). It has also been reported that thiourea is an effective antidote to herbicide toxicity (*35*). It can be concluded from this experiment that hyroxyl radical formation because of SDD−cystatin interaction is one of the prime factors responsible for SDD-induced cystatin damage. Thiol protease inhibitors play a major role in leaf senescence (*10*, *11*) and seed development. Moreover, cystatins purified from plant sources such as sugarcane can be employed to inhibit growth of filamentous fungus *Trichoderma reesi* (*13*). These inhibitors have also been shown to possess antiviral and antifungal activities. Thus, it is logical to think that any interactions resulting in the damage of protease inhibitor or any defect in cystatins regarding the loss of inhibitory activity, conformational change, or fragmentation may also affect the metabolic machinery of the plant. However, because of the fact that cystatins are present in the tubers (*36*), latex (*37*), and seeds (*38*) of plants, any damage to cystatin will be damaging the plant as a whole. Therefore, keeping in view the importance of cystatins and their presence in the mammalian system and plant kingdom, the study may be used as a model system to understand the interaction of plant and mammalian cystatins with SDD. Although, it is reported that 1 mM concentration of pesticide effects proteins (*2*), we have chosen a broader range (0.5−9 mM) to see the overall biochemical and biophysical changes in cystatins at varying concentrations and varying incubation times with fungicide SDD.

The studies on the interaction of SDD with cystatin provide significant evidence to prove the damage caused to the cystatin. At the present time, it can only be speculated that the mechanism involved in SDD-mediated fragmentation or conformational change in cystatin is certainly due to the suspected role of the hydroxyl radicals generated by SDD. These finding suggest that dithiocarbamates such as SDD deserve further attention because of their damaging effects.

ACKNOWLEDGMENT

Facilities provided by DRS operative in the Department of Biochemistry are thankfully acknowledged.

LITERATURE CITED

(1) Zilberman, D.; Schmitz, A.; Casterline, G.; Lichtenberg, E.; Siebert, J. B. The economics of pesticide use and regulation. *Science* **1991**, *253*, 518−522.

(2) Purcell, M.; Neault, J. F.; Malonga, H.; Arakawa, H.; Carpentier, R.; Tajmir-Riahi, H. A. Interactions of atrazine and 2,4-D with human serum albumin studied by gel and capillary electrophoresis, and FTIR spectroscopy. *Biochim. Biophys. Acta* **2001**, *1548*, 129−138.

(3) Baligar, P. N.; Kaliwal, B. B. Induction of gonadal toxicity to female rats after chronic exposure to mancozeb. *Ind. Health* **2001**, *39*, 253−243.

(4) Vaccari, A.; Saba, P.; Mocci, I.; Ruiu, S. Dithiocarbamate pesticides effect glutamate transport in brain synaptic vesicles. *Pharmacol. J. Exp. Ther.* **1997**, *288*, 1−5.

(5) Chauhan, L. K.; Saxena, P. N.; Gupta, S. K. Evaluation of cytogenetic effects of SDD on the root meristem cells of *Allium sativum*. *Biomed. Environ. Sci.* **2001**, *14*, 214−219.

(6) Xavier-Filho, J. Sementese suas defesas contra insetos. Projeto Multinacional de Biotecnologia e alimentos. *Organizacao dos Estados Americanas* **1992**, *1*, 31.

(7) Ryan, C. A. Proteinase inhibitor gene families: Strategies for transformation to improve plant defense against herbivores. *BioEssays* **1989**, *10*, 20.

(8) Solommon, M.; Belenghi, B.; Delledonne, M.; Menachen, E.; Levine, A. The involvement of cysteine proteinase and proteinases inhibitor genes in the regulation of programmed cell death in plants. *Plant Cell* **1999**, *11*, 431.

(9) Ceros, M.; Carbonell, J. Purification and characterization of thiol-protease induced during senescence of unpollinated ovaries of *Pisum sativum*. *Physiol. Plant* **1993**, *88*, 267−274.

(10) Greenberg, J. T. Programmed cell death: A way of life for plants. *Proc. Natl. Acad. Sci. U.S.A.* **1996**, *93*, 12094−12097.

(11) Lamb, C.; Dixon, R. A. The oxidative burst in plant disease resistance, Annu. Ver. Plant Physiol. *Plant Mol. Biol*. **1997**, *48*, 251−275.

(12) Machleidt, W.; Borchart, U.; Fritz, H.; Brzin, J.; Ritonja, A.; Turk, V. Protein inhibitors of cysteine proteinases. II. Primary structure of Stefin, a cytosolic protein inhibitor of cysteine proteinases from human polymorphonuclear granulocytes, Hoppe-Seyler's Z. *Physiol. Chem.* **1983**, *364*, 1481−1486.

(13) Ritonja, A.; Machleidt, W.; Barrett, A. J. Amino acid sequence of the intracellular cysteine proteinase inhibitor cystatin B from human liver. *Biochem. Biophys. Res. Commun.* **1985**, *131*, 1187−1192.

(14) Arai, S.; Matsumoto, I.; Abe, K. Phytocystatins and their target enzymes: From molecular biology to practical application: A review. *J. Food Biochem.* **1998**, *22*, 287−299.

(15) Abe, K.; Kondo, H.; Watanabe, H.; Emori, Y.; Arai, S. Oryzacystatins as the first well-defined cystatins of the plant origin and their target proteinases in rice seeds. *Biomed. Biochim. Acta* **1991**, *50*, 637−641.

(16) Barrett, A. J.; Fritz, H.; Grubb, A.; Isemura, S.; Javirnen, M.; Katunuma, N.; Machleidt, W.; Sasaki, M.; Turk, V. Nomenclature and classification of the proteins homologous with the cysteine proteinase inhibitor chicken cystatin. *Biochem. J.* **1986**, *236*, 312.

(17) Kondo, H.; Abe, K.; Emori, Y.; Arai, S. Gene organization of oryzacystatin II, a new cystatin superfamily member of plant origin, is closely associated to that of oryzacystatin I but different from those of animal cystatins. *FEBS Lett.* **1991**, *278*, 139−142.

(18) Aoki, H.; Akaike, T.; Abe, K.; Kuroda, M.; Arai, S.; Kamura, R. O.; Negi, A.; Maeda, H. Antiviral effect of oryzacystatin, a proteinases inhibitor in rice, against herpes simplex virus type I *in vitro* and *in vivo*. *Antimicrob. Agents Chemother*. **1995**, *39*, 846−849.

(19) Soares-Costa, A.; Beltramini, L. M.; Theimann, O. H.; Henrique-Silva, F. A sugarcane cystatin: Recombinant expression, purification, and antifungal activity. *Biochem. Biophys. Res. Commun*. **2002**, *296*, 1194−1199.

(20) Wu, J.; Norman Haard, F. Purification and characterization of cystatin from the leaves of methyl jasmonate treated tomato plants. *Comp. Biochem. Physiol., Part C: Pharmacol., Toxicol. Endocrinol.* **2000**, *127*, 209−220.

(21) Laemmli, U. K. Cleavage of structural proteins during the assembly of the head of bacteriophage T4. *Nature* **1970**, *227*, 680−685.

(22) Lowry, O. H.; Rosebrough, N. J.; Farr, A. J.; Randall, R. J. Protein measurement with Folin phenol reagent. *J. Biol. Chem.* **1951**, *193*, 265−275.

(23) Byler, D. M.; Susi, H. Examination of the secondary structure of proteins by deconvolved FTIR spectra. *Biopolymers* **1986**, *25*, 469−487.

(24) Elliot, A.; Ambrose, E. J. Spectroscopy in the 3 region of the infrared spectrum. *Nature* **1950**, *165*, 921−922.

(25) Timasheff, S. N.; Susi, H.; Stevens, L. Infrared spectra and protein conformation in aqueous solutions. *J. Biol. Chem.* **1967**, *242*, 5467−5473.

(26) Ruegg, M.; Metzger, V.; Susi, H. Computer analysis of characteristic infrared of globular proteins. *Biopolymers* **1975**, *14*, 1465−1471.

(27) Bramanti, E.; Benedetti, E. Determination of the secondary structure of isomeric forms of human serum albumin by a particular frequency deconvulation procedure applied to Fourier transform IR analysis. *Biopolymers* **1996**, *38*, 639−653.

(28) Krimm, S.; Bandekar, J. Vibrational spectroscopy and conformation of peptides, polypeptides, and proteins. *Adv. Protein Chem*. **1986**, *38*, 181−236.

(29) Miyazawa, T.; Blout, E. R. The infrared spectra of polypeptides in various conformations: Amide I and amide II bands. *J. Am. Chem. Soc*. **1961**, *83*, 712−719.

(30) Surewicz, W. K.; Moscarello, M. A.; Mantsch, H. H. Secondary structure of the hydrophobic myelin protein in a lipid environment as determined by Fourier transform infrared spectroscopy. *J. Biol. Chem.* **1987**, *262*, 8598−8602.

(31) Kelner, M. J.; Bagnell, R.; Welch, K. J. Thioureas react with super oxide radicals to yield a sulfhydryl compound: Explanation of protective effect against paraquat. *J. Biol. Chem.* **1990**, *265*, 1306−1311.

(32) Becana, M.; Moran, J. F.; Iturbe-Ormaetxe, I. Iron-dependent oxygen free radical generation in plants subjected to environmental stress: Toxicity and antioxidant protection. *Plant Soil* **1998**, *201*, 137−147.

(33) Reddy, N. R.; Salunkhe, D. K.; Sathe, S. K. Biochemistry of Black Gram (*Phaseolus mungo L.*): A review. *Crit. Rev. Food Sci. Nutr*. **1982**, *58*, 49−112.

(34) Schopfer, P.; Plachy, C.; Frahry, G. Release of reactive oxygen intermediates (superoxide radicals, hydrogen peroxide, and hydroxyl radicals) and peroxidase in germinating radish seeds controlled by light, gibberellin, and abscisic acid. *Plant Physiol.* **2001**, *125*, 1591−1602.

(35) Trebst, A.; Depka, B.; Cytzko, H. A Specific role for Tocopherol and of singlet oxygen quenchers in the maintenance of photosystem II, structure and function in *Chlamydomonas reinhardtii*. *FEBS Lett*. **2000**, *516*, 156−160.

(36) Waldron, C.; Wegrich, L. M.; Owens, Metro, P. A.; Walsh, T. A. Characterization of a genomic sequence coding for potato multicystatin, of eight domain cystein proteinase inhibitor. *Plant Mol. Biol*. **1993**, *23*, 801−812.

(37) Monti, R.; Contiero, J.; Goulart, A. J. Isolation of natural inhibitors of papain obtained from *Carica papaya* latex. *Braz. Arch. Biol. Technol.* **2004**, *47*, 747−754.

(38) Oliveira, A. S.; Pereira, R. A.; Lima, L. M.; Morais, A. H. A.; Melo, F. R.; Franco, O. L.; Bloch, C., Jr.; Grossi-de-sa, M. F.; Sales, M. P. Activity toward Bruchid pest of a Kunitz type inhibitor from seeds of the Algaroba tree (*Prosopis juliflora* D.C.). *Pestic. Biochem. Physiol.* **2002**, *72*, 122−132.

Received for review March 15, 2005. Revised manuscript received June 2, 2005. Accepted June 6, 2005.

JF050580P